ACCOUNTS
of chemical research

Redox Tuning over Almost 1 V in a Structurally Conserved Active Site: Lessons from Fe-Containing Superoxide Dismutase

ANNE-FRANCES MILLER*

Department of Chemistry, University of Kentucky, Lexington, Kentucky 40506-0055, and Departments of Chemistry and Biophysics, The Johns Hopkins University, Baltimore, Maryland 21218

RECEIVED ON NOVEMBER 2, 2007

CONSPECTUS

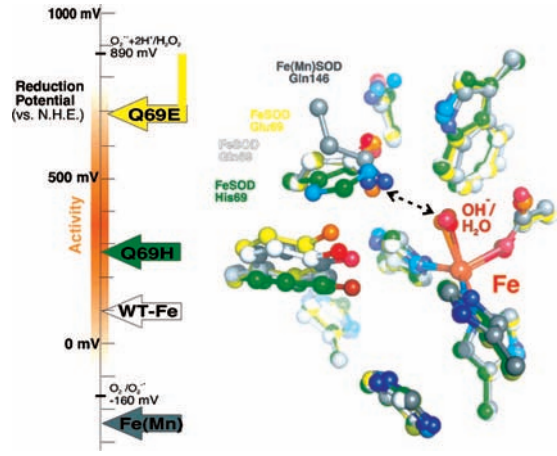

Metalloenzymes catalyze some of the most demanding reactions in biochemistry, thereby enabling organisms to extract energy from redox reactions and utilize inorganic starting materials such as N_2 and CH_4. Bound metal ions bring to enzymes greater chemical versatility and reactivity than would be possible from amino acids alone. However the host proteins must control this broad reactivity, activating the metal for the intended reaction while excluding the rest of its chemical repertoire. To this end, metalloproteins must control the metal ion reduction midpoint potential (E_m), because the E_m determines what redox reactions are possible. We have documented potent redox tuning in Fe- and Mn-containing superoxide dismutases (FeSODs and MnSODs), and manipulated it to generate FeSOD variants with E_ms spanning 900 mV (21 kcal/mol or 87 kJ/mol) with retention of overall structure. This achievement demonstrates possibilities and strategies with great promise for efforts to design or modify catalytic metal sites.

FeSODs and MnSODs oxidize and reduce superoxide in alternating reactions that are coupled to proton transfer, wherein the metal site is believed to cycle between $M^{3+}\cdot OH^-$ and $M^{2+}\cdot OH_2$ (M = Fe or Mn). Thus the E_m reflects the ease both of reducing the metal ion and of protonating the coordinated solvent molecule. Moreover similar E_ms are achieved by Fe-specific and Mn-specific SODs despite the very different intrinsic E_ms of high-spin $Fe^{3+/2+}$ and $Mn^{3+/2+}$. We provide evidence that E_m depression by some 300 mV can be achieved via a key enforced H-bond that appears able to disfavor proton acquisition by coordinated solvent. Based on ^{15}N-nuclear magnetic resonance (NMR), stronger H-bond donation to coordinated solvent can explain the greater redox depression achieved by the Mn-specific SOD protein compared with the Fe-specific protein. Furthermore, by manipulating the strength and polarity of this one H-bond, with comparatively minor perturbation to active site atomic and electronic structure, we succeeded in raising the E_m of FeSOD by more than 660 mV, apparently by a combination of promoting protonation of coordinated solvent and providing an energetically favorable source of a redox-coupled proton. These studies have combined the use of electron paramagnetic resonance (EPR), NMR, magnetic circular dichroism (MCD), and optical spectrophotometry to characterize the electronic structures of the various metal sites, with complementary density functional theoretical (DFT) calculations, NMR spectroscopy, and X-ray crystallography to define the protein structures and protonation states. Overall, we have generated structurally homologous Fe sites that span some 900 mV, and have demonstrated the enormous redox tuning accessible via the energies associated with proton transfer coupled to electron transfer. In this regard, we note the possible significance of coordinated solvent molecules in numerous biological redox-active metal sites besides that of SOD.

Published on the Web 04/01/2008 www.pubs.acs.org/acr
10.1021/ar700237u CCC: $40.75

Introduction to FeSOD and MnSOD

Superoxide dismutases (SODs) catalyze the disproportionation of superoxide to molecular oxygen and hydrogen peroxide, as part of cells' defense against oxidative stress.[1] SODs are found in all aerobic organisms, and their activity modulates the consequences and courses of numerous conditions including inflammation, diabetes, neuronal degeneration, cancer, and old age. Three different enzymes all share the name SOD because they catalyze the same overall reaction. The Cu- and Zn-containing SODs are generally eukaryotic. Ni-containing SODs are found in certain fungi and bacteria, and the Fe- or Mn-dependent SODs (Fe/MnSODs) are found predominantly in bacteria, some plant chloroplasts (FeSOD), and mitochondria (MnSOD). Fe- and MnSODs share structural[2] and amino acid sequence homology[3] and are therefore considered to constitute a single class of SODs. Some members of this class display significant activity with either Mn or Fe (cambialistic Fe/MnSODs),[4,5] whereas others are active only with Fe (FeSODs) or Mn (MnSODs).

Fe/MnSODs are dimers or tetramers of identical ~22 kDa monomers, each with an active site containing a single Mn or Fe ion (Figure 1). The metal ion adopts trigonal bipyramidal geometry, bound by two histidines and one aspartate ligand in the equatorial plane. A third histidine plus a molecule of coordinated solvent serve as axial ligands. Figure 1 also shows a crystallographic water molecule in the channel that provides access to solvent, at the position from which substrate and analogous exogenous anions such as N_3^- are believed to bind to Fe^{3+}.[6]

Fe or Mn reduction is coupled to proton uptake,[7,8] most likely by the coordinated solvent, so the metal center cycles between $M^{3+}\cdot OH^-$ and $M^{2+}\cdot H_2O$, for M = Fe or Mn.[9,10] Thus, Fe/MnSODs alternately oxidize and reduce $O_2^{\bullet-}$, and protonate substrate in the rate limiting step (eq 1b):[7]

$$O_2^{\bullet-} + H^+ + LM^{3+}\cdot OH^- \rightarrow O_2 + LM^{2+}\cdot OH_2 \quad (1a)$$

$$O_2^{\bullet-} + H^+ + LM^{2+}\cdot OH_2 \rightarrow H_2O_2 + LM^{3+}\cdot OH^- \quad (1b)$$

where L stands for the SOD protein.[7–9]

The coordinated solvent hydrogen bonds (H-bonds) with a second sphere residue, which is either a glutamine or a histidine, and this is the coordinated solvent's only interaction beyond the metal ion coordination sphere (Figure 1).[6,11] The glutamine in turn H-bonds with the conserved Tyr34, Asn72, and Trp122 (Figure 1) in a H-bond network that extends over both domains of the protein, thus allowing any energy associated with the H-bond to solvent to be distributed over distant elements of the protein structure. Because glutamine's H-bond with Trp122 must constitute H-bond acceptance by glutamine, this constrains the glutamine's side chain O to present its $-NH_2$ group in H-bond *donation* to coordinated solvent. Among mesophilic FeSODs, the glutamine derives from position 69, whereas the analogous glutamine of MnSODs derives from position 146 (Figure 1, numbering is based on the FeSOD and MnSOD of *E. coli*).[12,13]

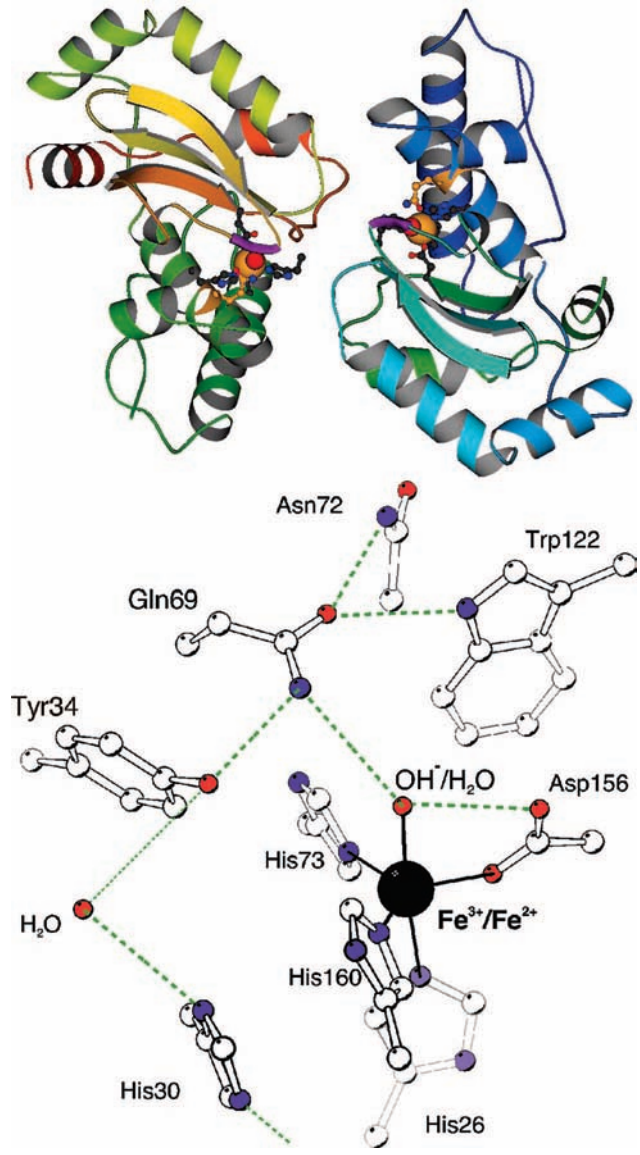

FIGURE 1. Ribbon structure of FeSOD and cartoon view of the active site, based on the 1ISB.pdb coordinates of Lah et al.[6] The ribbon structure shows the position of the active site glutamine of FeSOD (orange) and MnSOD (purple, backbone only). Green dashed lines indicate H-bonds present in the active sites of at least some FeSOD variants.

Early Metal Ion Substitutions. Brock, Harris, Ose, and Fridovich showed that MnSOD depleted of Mn and reconstituted with Fe lacked activity.[15–16] Similarly, Yamakura showed that

FeSOD is not active with Mn bound,[17] and mis-incorporation of Fe into mitochondrial (Mn)SOD protein results in an inactive SOD.[18] In contrast, cambialistic Fe/MnSODs can use either metal ion.[4,5] Given the thousands of Fe/MnSODs that exist, it is most likely that they will span a range of specificities for Fe vs Mn. Nevertheless, Fe/MnSODs with the highest specific activities with one metal ion appear essentially inactive with the other.

We proposed that the relative inactivity of Fe-substituted MnSOD and Mn-substituted FeSOD (Fe(Mn)SOD and Mn(Fe)-SOD, respectively) could be substantially due to differences in the redox tuning applied by Fe-specific vs Mn-specific proteins, which would be appropriate for the native metal ion but not the other.[19] Under this hypothesis, the cambialistic Fe/Mn-SODs would apply intermediate redox tuning that would enable either metal ion to function.

The electronic configurations of high-spin Fe and Mn produce very different reduction midpoint potentials (E_ms) for the 3+/2+ couple. For d^4 Mn^{3+}, the electron acquired upon reduction is readily accommodated in a vacant d orbital. However for d^5 Fe^{3+}, reduction requires that one orbital accommodate a second electron. Thus, for the hexa-aquo ions, the 3+/2+ E_ms are reported as 1.5 and 0.77 V vs the normal hydrogen electron (NHE) for Mn and Fe, respectively.[20] Similarly, for the Mn− and Fe−EDTA complexes, they are 0.8 and 0.1 V vs NHE, respectively.[21] Borovik's group finds that for complexes with tripodal tris[(*N*′-*tert*-butylureaylato)-*N*-ethyl]aminato ligands, the Mn−hydroxide complex has an E_m 300 mV higher than that of the analogous Fe complex.[22] Thus, one anticipates that if bound by a protein in the same way, $Mn^{3+/2+}$ should display an E_m several hundred millivolts higher than that of $Fe^{3+/2+}$. However optimal SOD activity requires E_m values intermediate between the potentials of the two half-reactions.[23] Thus, we reasoned that the Mn-specific SOD protein ((Mn)SOD) should depress the E_m of its bound metal ion several hundred millivolts more than should the Fe-specific SOD protein ((Fe)SOD, Figure 2).[19] By extension, we proposed that when (low E_m) Fe is bound in (depressing) (Mn)SOD protein, the resulting Fe(Mn)SOD should have an E_m several hundred millivolts lower than that of FeSOD (Figure 2, right) and that the E_m of Mn(Fe)SOD would be much higher than that of MnSOD (Figure 2, left). Similarly, we proposed that the above mis-metalated SODs should fail to turn over due to inability to oxidize or reduce superoxide, respectively.[19]

This was proven to be correct for the SODs of *Escherichia coli*.[19,24] Fe(Mn)SOD was found to display negligible activity at neutral pH and an E_m near −240 mV vs NHE, whereas analogous titrations of FeSOD displayed reversible Nerstian behavior with an E_m of 220 mV,[19] close to results obtained by other groups.[23] Even comparison with more recent titrations that obtain 20 mV for FeSOD,[25] yields an ~300 mV lower E_m for Fe in Fe(Mn)SOD vs FeSOD.[19] Similarly, MnSOD was found to have an E_m near 290 mV (vs. 390 mV for human MnSOD[26]) whereas oxidation of Mn(Fe)SOD required the use of the strong oxidant MnO_4^- ($E_m \approx 1.5$ V).[24] Even $IrCl_6^{2-}$ ($E_m \approx 0.87$ V) or $MoCN_8^{3-}$ ($E_m \approx 0.82$ V)[20] proved unable to oxidize Mn(Fe)SOD. Thus, the E_m of Mn(Fe)SOD could be estimated to lie above 930 mV, representing a >0.5 V increase above the E_m of MnSOD.[19]

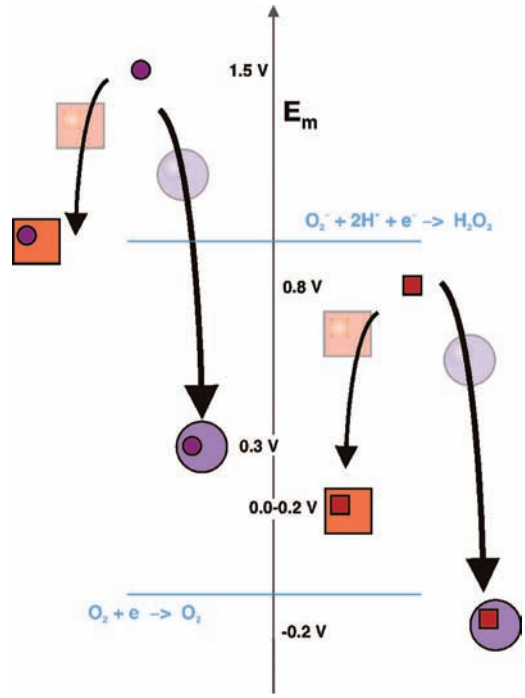

FIGURE 2. Model for different redox tuning applied by the Fe-specific SOD protein (orange) and the Mn-specific SOD protein (violet) upon Fe (red) and Mn (purple). Potentials are vs NHE and those of superoxide's reactions are from Sawyer and Valentine.[45]

Such large displacements of E_m suffice to explain the inabilities of Fe(Mn)SOD and Mn(Fe)SOD to turn over at a significant rate. Furthermore, Fe(Mn)SOD retained ability to bind and reduce superoxide but specifically lacked ability to oxidize it, consistent with Fe(Mn)SOD's low E_m. Moreover additional factors that may contribute to the inactivities of Fe(Mn)SOD and Mn(Fe)SOD likely stem from the same active site differences that are responsible for the different E_ms. Fe^{3+}(Mn)SOD retained N_3^-, F^-, and OH^- binding affinities actually slightly higher than those of Fe^{3+}SOD.[27] Fe^{3+}(Mn)SOD might therefore be susceptible to competitive inhibition by OH^- at neutral pH, and indeed activity is restored to a small (7%) but significant extent at lower pH.[28,29] However because other small anions also bind with heightened affinity, it is reason-

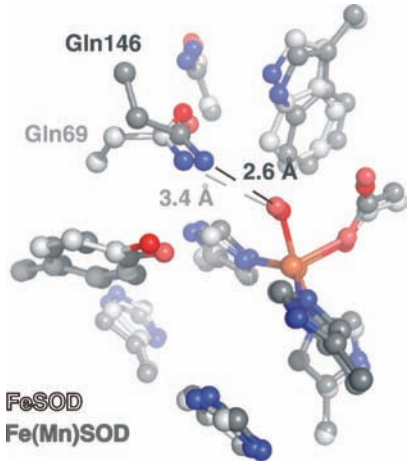

FIGURE 3. Overlay of the active sites of *E. coli* FeSOD (light gray, 1ISB.pdb) and Fe(Mn)SOD (dark gray, site A in Edwards' coordinates 1MMM.pdb). An additional OH^- is coordinated to Fe^{3+} in site B, consistent with the p*K* for OH^- binding of 6–7[27,29,46] and the pH of 8.5 used for crystallization.[30] Figure generated using PyMOL.[47]

able to expect that $O_2^{\bullet-}$ may too, so information on *specificity* is needed. Moreover, recovery of activity at lower pH (near 6) is also consistent with our proposal that a low E_m can explain Fe(Mn)SOD's inactivity. For reduction coupled to proton uptake, the E_m is expected to rise at lower pHs; thus Fe(Mn)SOD's E_m is expected to approach the value required for oxidation of $O_2^{\bullet-}$,[19] with concomitant recovery of activity, at low pH.

Mn^{2+}(Fe)SOD did not bind N_3^- or F^-.[24] Thus its inability to reduce $O_2^{\bullet-}$ may reflect substrate binding defects additional to its very high E_m. However the limits we have placed on Mn(Fe)SOD's E_m suffice to explain its inactivity.

Why Are the Midpoint Potentials so Different? The 1.8 Å-resolution crystal structure of Fe(Mn)SOD does not reveal an obvious structural basis for the low activity and E_m of Fe in the (Mn)SOD protein (Figure 3).[30] Electronic structural differences sufficient to cause the altered E_ms of Fe when bound in (Mn)SOD protein are also not observed. The EPR signal is very sensitive to the coordination environment of Fe^{3+} and detects subtle differences between the *g* values of Fe^{3+}SOD and Fe^{3+}(Mn)SOD for the turning points attributable to the $m_s = \pm 3/2$ Kramer's doublet, yielding zero-field parameters of $|D| = 1.85\ cm^{-1}$, $E/|D| = 0.24$, and $|D| = 2\ cm^{-1}$, $E/|D| = 0.22$, respectively. Thus, Fe^{3+} appears to experience similar ligand fields in the (Mn)SOD and (Fe)SOD proteins. Likewise, the paramagnetic contributions to chemical shift report on covalency of ligand coordination to Fe^{2+}, as well as anisotropy of the unpaired electron spin density distribution.[31,32] Hence the similarity of the ^1H chemical shifts of the histidine ligands of Fe^{2+} near 88, 43, and 36 ppm in Fe^{2+}(Mn)SOD and Fe^{2+}SOD indicates that the Fe^{2+} electronic structure is not very different for

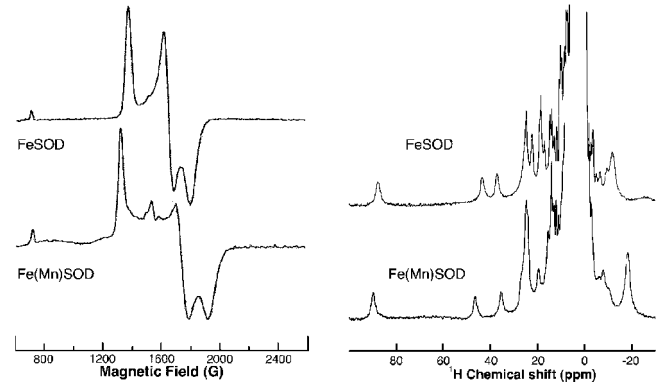

FIGURE 4. X-band EPR spectra (left) obtained at 70 K on samples buffered at approximately pH 7.6 with 50 mM potassium phosphate and 50 mM KCl, and ^1H NMR spectra (right) of Fe^{2+}(Mn)SOD and Fe^{2+}SOD obtained at 30 °C on samples buffered at pH 6.7 and 7.2, respectively, with 100 mM potassium phosphate.[27]

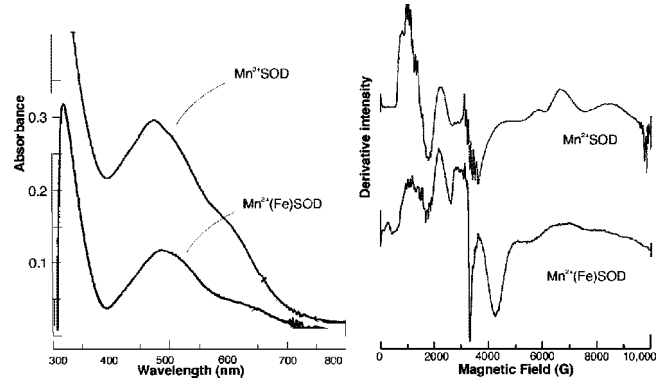

FIGURE 5. Optical spectra (left) of Mn^{3+}SOD and more dilute Mn^{3+}(Fe)SOD oxidized with substoichiometric $KMnO_4$ in 100 mM potassium phosphate buffer at pH 7.8, and EPR spectra (right) of Mn^{2+}SOD and Mn^{2+}(Fe)SOD buffered with 50 mM potassium phosphate at pH 7.8 and 50 mM NaCl. Some free Mn^{2+} is evident in the MnSOD sample, which was reduced with H_2O_2.[24]

Fe^{2+} bound in (Fe)SOD vs (Mn)SOD (Figure 4). Recent magnetic circular dichroism (MCD) and computational studies by Brunold's team confirm this.[33a]

Interestingly however, the EPR spectra of the azide and OH^- complexes of Fe^{3+}SOD and Fe^{3+}(Mn)SOD differ significantly, hinting at differences in substrate binding modes or polarization in the two proteins[27] (and more recently[33b]).

The electronic states of Mn^{2+} and Mn^{3+} also appear alike in Mn(Fe)SOD and MnSOD (Figure 5). Based on the optical spectra of Mn^{3+}SOD and Mn^{3+}(Fe)SOD, the two Mn^{3+} sites are similar. For Mn^{2+}, X-band EPR indicates subtle differences that may correlate with E_m, as revealed by the appearance of a "zero-field" transition near 300 G in the EPR spectrum of Mn^{2+}(Fe)SOD but not in that of Mn^{2+}SOD; however, simulations and spectroscopy at additional fields are needed in order to obtain detailed understanding (e.g., see work by Un et

al.).[34] Overall, despite the complexity stemming from comparable zero-field and Zeeman transition energies, the presence of analogous features in similar positions indicates that the Mn^{2+} ions experience similar coordination environments in the two proteins. Thus, altered electronic structures do not appear to be the primary source of the much lower E_ms produced by (Mn)SOD vs (Fe)SOD protein. Moreover, the finding that both Fe and Mn have a much lower E_m when bound to (Mn)SOD indicates that asymmetry of the coordination sphere is unlikely to be the basis for redox tuning, because the 3+ state of Mn would be strongly favored by Jahn–Teller distortion but that of Fe would not.

Labile Protons: Differences in *E. coli* FeSOD vs MnSOD May Complement the Different Metal Ions

Labile protons play several roles in the mechanism of SOD, including activating superoxide for reduction, displacing the metal ion from product, and possibly forestalling formation of the inhibited complex of MnSOD. One proton can be transferred directly or indirectly from coordinated H_2O to substrate, in conjunction with electron transfer from the metal ion to substrate. In addition, Tyr34 and Gln69 have been proposed to play roles in transfer of protons between the coordinated solvent, bulk solvent, and substrate (see numerous works by Silverman and Whittaker). The p*K*′s of Tyr34 thus form an element of catalytic competence; they also report on the polarization of the active site H-bond network (distribution of charge) and thus illuminate differences between the two proteins that may complement and compensate for properties of the metal ion, and thus contribute to metal ion specificity.

The p*K* of 8.5 of Fe^{2+}SOD was assigned to Tyr34 based on direct observation of [$^{13}C^{\zeta}$]-tyrosine by ^{13}C-NMR vs pH.[8] In Fe^{3+}SOD however, the p*K* reflects more favorable OH^- binding to Fe^{3+}, which apparently suppresses ionization of Tyr34.[35] In contrast, the p*K* near 9.5 of Mn^{3+}SOD was assigned to ionization of Tyr34, consistent with the Jahn–Teller stabilization enjoyed by pentacoordinate (d^4) Mn^{3+}, which would be lost upon binding of OH^-.Mn^{2+} Thus, the metal ion identity plays an important role in determining how the active site accommodates changes in availability of labile H^+ and OH^-, despite the presence of the same amino acids. In order to provide protons with similar p*K*′s for the SOD reaction, the two proteins must therefore employ subtly different mechanisms or apply different tuning to the p*K*′s of the amino acids. Indeed, the p*K* of Fe^{3+}(Mn)SOD for coordination of OH^- to Fe^{3+} is some two pH units lower than that of Fe^{3+}SOD,[46] indicating that the (Mn)SOD protein favors anion binding more than does (Fe)SOD, and Fe(Mn)SOD may not release product as readily as FeSOD. Similarly, Mn^{3+} bound in (Fe)SOD may fail to bind substrate.

While the p*K* of Fe^{2+}SOD of 8.5 is assigned to Tyr34, the reduced-state p*K* of Mn^{2+}SOD appears to be more complex, apparently involving Tyr34 and possibly either deprotonation of coordinated H_2O or coordination of a second OH^-, consistent with the greater tendency of Mn^{2+} than Fe^{2+} to acquire harder ligands and adopt a six-coordinate geometry. Although treatment at high pH ultimately results in Mn^{2+} release,[34] a new species is also observed in the Mn^{2+}SOD EPR spectrum near $g' \approx 4.17$.[35] Its Mn^{2+}EDTA–like signal accompanied by only minor formation of the sharp $g' = 2$ signal associated with Mn^{2+} release suggests coordination of exogenous OH^- to Mn^{2+} in a sequence that could initially increase the Mn^{2+} coordination number but also progress to displacement of protein ligands, thus freeing Mn^{2+} from specific well–defined binding in the active site.[34]

Proposal: Protonation of Coordinated Solvent Is Suppressed in *E. coli* MnSOD by Stronger H-Bond Donation. We proposed that the different E_ms produced by the (Fe)SOD and (Mn)SOD proteins could be substantially explained by different extents of protonation of coordinated solvent (different p*K*′s).[19] There is inorganic precedent for E_m shifts over many hundreds of millivolts upon ligand protonation,[36] and computational models of SOD indicate a possible 1.3 V effect of protonating coordinated solvent.[37] Thus, this mechanism is capable of explaining the large effect we observe. In addition, insofar as coordinated solvent is the redox-coupled proton acceptor, its oxidized- and reduced-state p*K*′s will contribute to the E_m (Scheme 1). Finally, coordinated solvent's only contact outside the metal site is Gln69, the most highly conserved difference between Fe-specific and Mn-specific SODs, so our proposal makes chemical sense of biological correlations.[38] Given the different positions of the glutamines of FeSOD vs MnSOD, it is reasonable to propose that they could depress the coordinated solvent's p*K*′s to different extents, and if the active site of (Mn)SOD suppresses proton uptake, reduction too will be suppressed, producing a depressed E_m, as observed. There are numerous precedents for p*K* tuning over 5 pH units, which would produce an E_m change of 300 mV based on a single p*K*. Moreover additional contributions could further modulate the E_m, such as the source and destination of the redox-coupled proton (below).

If (Mn)SOD protein lowers the E_m by suppressing proton acceptance by coordinated solvent, then glutamine's H-bond donation to coordinated solvent should be stron-

SCHEME 1. Proton-Coupled Reduction of Fe in SOD and its Contribution to the Measured E_m[a]

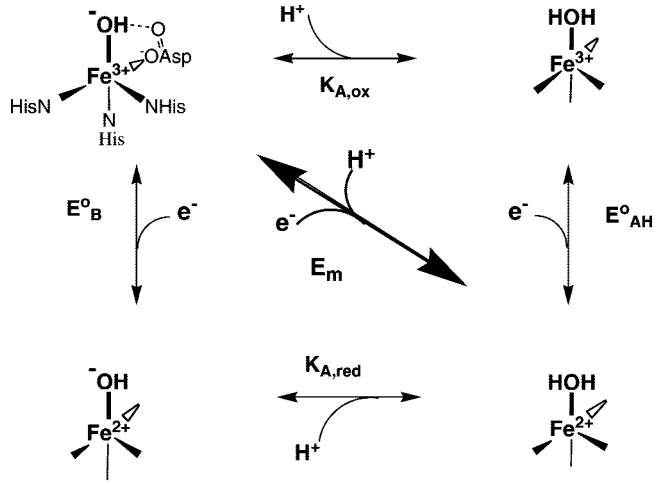

$$E_m = E^o{}_{AH} + \frac{RT}{F}\ln\frac{K_{A,red} + [H^+]}{K_{A,ox} + [H^+]}$$

[a] Protein ligands are shown in upper left quadrant but omitted elsewhere, for clarity.

ger in (Mn)SOD than in (Fe)SOD. This prediction was borne out by ^{15}N NMR of the glutamine side chains of Fe^{2+}SOD and Fe^{2+}(Mn)SOD (Figure 6). In Fe^{2+}SOD, the side-chain N of Gln69 displayed a 45 ppm paramagnetic shift from the chemical shift typical of diamagnetic glutamine side chains.[39] This paramagnetic shift provides a measure of the proximity of the glutamine side chain N to Fe^{2+}, as well as its coupling to Fe^{2+} via H-bonding to coordinated solvent. In Fe^{2+}(Mn)SOD, an analogous resonance was identified, again in selectively labeled samples, however with a paramagnetic shift of 79 ppm.[40] Thus, the side chain N of Gln146 in Fe^{2+}(Mn)SOD is significantly more strongly coupled to Fe^{2+}.[40] While we have not separated the through-space and through-bond contributions to the paramagnetic shift, a shorter distance is expected for a stronger H-bond to coordinated solvent, so either interpretation indicates significantly stronger H-bond donation to coordinated solvent in Fe^{2+}(Mn)SOD than in Fe^{2+}SOD, consistent with stronger suppression of proton uptake by coordinated solvent in the (Mn)SOD protein.

The (Amino) Acid Tests: Q69H and Q69E FeSOD

To distinguish a cause-and-effect relationship from a possible common cause, we made amino acid substitutions designed to decrease the strength of H-bond donation to coordinated solvent (Q69H) or to reverse the polarity of H-bonding (Q69E). Our model predicts that *weakened H-bond donation* should relieve E_m depression, whereas H-bond *acceptance* should *actively raise* the E_m. Indeed, Q69H FeSOD displays an E_m some 250 mV higher than that of WT FeSOD.[25] Remarkably, the E_m of Q69E FeSOD appears to be >660 mV higher than that of WT FeSOD. The measured E_ms suffice to explain the observed decreases in activity,[25] although additional consequences of these substitutions are evident, for Q69E FeSOD in particular. Thus, although the E_ms of Q69H and Q69E FeSOD are consistent with redox tuning via modulation of the strength and polarity of H-bonding to coordinated solvent and more generally the energy associated with redox-coupled proton uptake, we first address alternative possible bases for the altered E_ms.

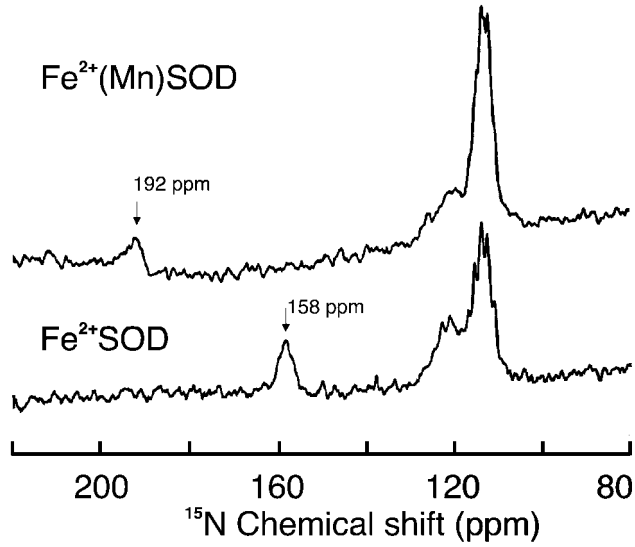

FIGURE 6. ^{15}N NMR spectra of Fe^{2+}SOD and Fe^{2+}(Mn)SOD selectively ^{15}N-labeled in glutamine side chains. Samples were buffered at pH 7.6 with 100 mM potassium phosphate, reduced with a slight excess of dithionite, and flame-sealed.[40]

Atomic Structure. To assess possible protein structural changes, we solved the crystal structures of both mutant SODs and found them to be essentially superimposable on the WT structure.[25] Backbone C^α RMSDs between the mutant and the WT were 1.3 and 0.7 Å, for Q69H and Q69E FeSOD, respectively. In Q69H FeSOD, Tyr34 was slightly displaced toward the solvent channel, presumably due the greater bulk of histidine than glutamine (Figure 7). Importantly, although His69 retained a 3.4 Å H-bond with coordinated solvent, the altered orientation of the His69 side chain resulted in loss of the H-bonds with Trp122, Asp72, and Tyr34 that characterize Gln69 in WT FeSOD. Thus, His69 is not constrained by the protein to act as an H-bond donor to coordinated solvent but could act as an H-bond acceptor instead, if neutral. Otherwise, both crystal structures concur that gross disruption of the pro-

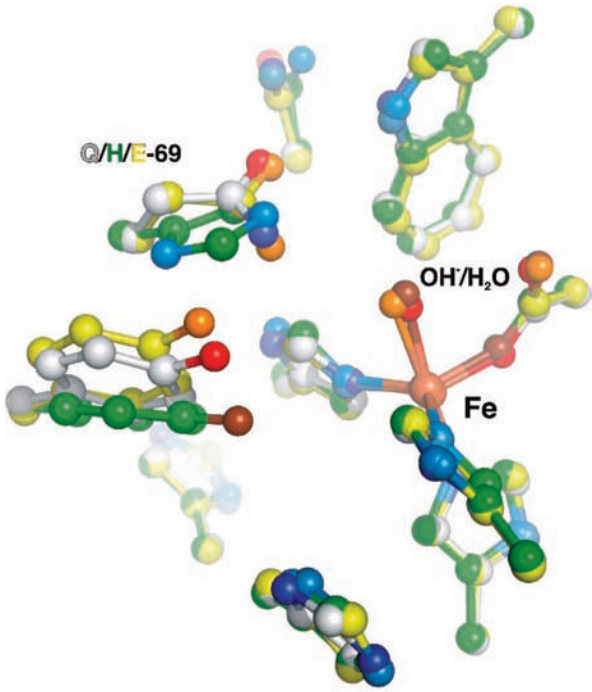

FIGURE 7. Overlay of the active sites of WT FeSOD (white), Q69H FeSOD (green), and Q69E FeSOD (yellow). Overlays were based on the side chains of residues 26, 30, 31, 34, 72, 73, 122, 156, 158, 159, 160, and 161 and performed in SwissPDBviewer (http://ca.expasy.org/spdbv/). Figure generated using PyMOL.[47]

tein and active site structure is unlikely to be the origin of the strongly elevated E_ms of Q69H and Q69E FeSOD.

Electronic Structure. Altered Fe^{3+} or Fe^{2+} electronic structures in the mutants would provide an excellent explanation for the altered E_ms; however this was not observed. The Fe^{2+} sites of Q69H and Q69E Fe^{2+}SOD were compared with that of Fe^{2+}SOD via the paramagnetically shifted ^{1}H resonances of the ligand histidines. Because these displayed very similar chemical shifts in all three cases, it appears that the anisotropy of unpaired electron spin density (orbitals and occupancy), as well as the geometry of the sites, are similar.[41] Similarly, MCD, optical, and EPR spectroscopies concur that the Q69H mutant retains a WT-like Fe^{3+} electronic structure.[41] The Q69E mutation produced a striking change in the EPR signal, to one resembling that formed upon OH^- binding to WT Fe^{3+}SOD at high pH (Figure 8).[42] MCD spectroscopy discerns a six-coordinate population that resembles high-pH WT FeSOD in addition to a pentacoordinate WT-like population at lower pHs.[33,43] Thus, the electronic structure of Fe^{3+} appears similar in analogous states of Q69E Fe^{3+}SOD and WT Fe^{3+}SOD, but Q69E Fe^{3+}SOD has a higher affinity for an exogenous anion, likely OH^-. Because binding of the sixth ligand is spontaneous, it must stabilize the oxidized site and cannot be a source of Q69E FeSOD's elevated E_m.

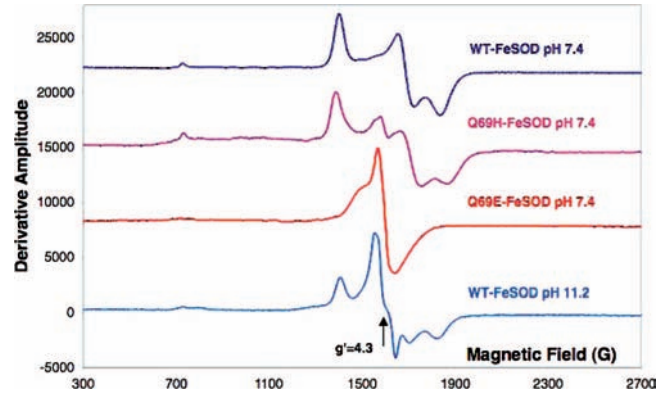

FIGURE 8. EPR spectra of mutant Fe^{3+}SODs compared with WT FeSOD at neutral and high pH. Samples were buffered with 100 mM PIPES (Q69H and WT FeSOD) or 50 mM potassium phosphate (Q69E FeSOD). The latter was chemically oxidized using $KMnO_4$ and frozen immediately.[41]

Protonation States and Hydrogen Bonding. The nature of H-bonding between His69 and coordinated solvent depends on whether His69 is cationic (obligate H-bond donor) or neutral (donor or acceptor). The WT-like p*K*'s for ionization of Tyr34 in the reduced state and OH^- binding to the oxidized state indicate that His69 is like Gln69, neutral, in both oxidation states. Additionally, the strong similarity of the EPR and ^{1}H NMR spectra of Q69H and WT Fe^{3+}SOD indicate that the ligand histidines and coordinated solvent have the same protonation states in the Q69H mutant as in WT. Therefore, it is simplest to conclude that labile protons are distributed similarly in the two active sites and therefore that coordinated solvent acquires a proton upon Fe reduction, as in WT. However, the absence of H-bonding constraints on His69 allows that His69 can act as an H-bond acceptor when H-bond donation is unfavorable. Thus Q69H FeSOD's higher E_m than WT FeSOD can be attributed to loss of enforced H-bond donation.

For Q69E FeSOD, the oxidized state's elevated affinity for exogenous anions argues that Glu69 is not anionic. This is most reasonable chemically, because ionization of Glu69 would place a negative charge immediately adjacent to coordinated OH^- (Figure 7).[44] For the reduced state, pH titrations indicate that deprotonation of Tyr34 is suppressed, rather than favored as in WT FeSOD, indicating the presence of an extra anion in the Q69E active site. If Glu69 does indeed change from neutral to anionic in conjunction with Fe reduction, then it is a redox-coupled proton donor, unlike the WT glutamine it replaces (Scheme 2). The WT-like paramagnetically dispersed ^{1}H NMR spectrum most simply suggests coordinated H_2O as in WT Fe^{2+}SOD, and the oxidized state most likely has coordinated OH^- based on extensive inorganic precedent.[44] Thus, we retain presumed redox-coupled proton acquisition by

SCHEME 2. Comparison of Proposed Proton-Coupled Electron Transfer in Q69E FeSOD (top) with That Accepted for WT FeSOD (bottom)

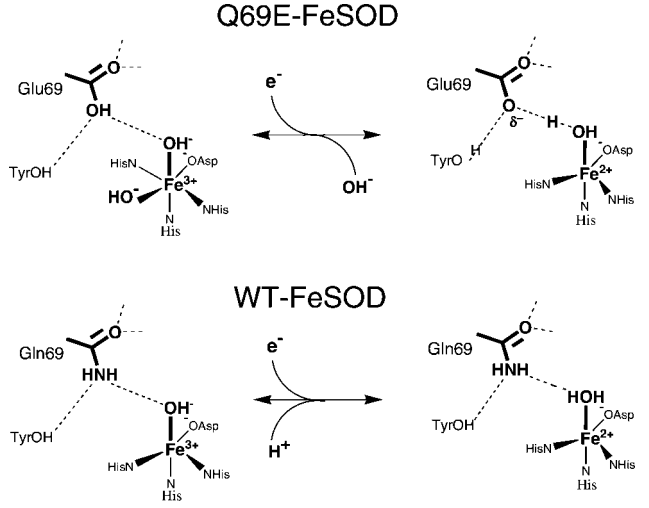

coordinated solvent and propose net transfer of a proton from Glu69 to coordinated OH^- upon reduction of Fe^{3+}, consistent with literature p*K*'s for glutamic acid and solvent coordinated to Fe^{3+} or Fe^{2+}.[44]

Because the data in hand suggested that Glu69 could play an active role in redox-coupled proton transfer that is new to the Q69E mutant, we sought more direct evidence on the protonation state and H-bonding of Glu69. Borgstahl and her team solved a new X-ray crystal structure of Q69E Fe^{2+}SOD based on 1.1 Å resolution crystallographic data.[41] The glutamic acid side chain C−O distances were compared after refinement vs two different models, one in which Glu69 was assumed to be neutral and another in which Glu69 was assumed to be ionized. The results suggested that Glu69 is significantly polarized, such that the O atom nearest coordinated solvent has a longer C−O bond than does the O nearer Trp122 and Asn72 (Figure 7).[41] This was best explained on the basis of anionic Glu69 with strong H-bonding from coordinated H_2O and neutral Tyr34 on the basis of DFT calculations as well as residual electron density suggestive of possible proton sharing among these three residues.[41] We found that regardless of whether the extra negative charge of the Q69E Fe^{2+}SOD active site was placed on Glu69, Tyr34, coordinated solvent, or even an additional molecule of solvent in the substrate access channel, only Glu69 was recovered as an anion upon energy minimization.[41] These calculations not only computationally document proton transfer from Glu69 to coordinated solvent upon Fe reduction in Q69E FeSOD but affirm that Glu69 is anionic and acts as an H-bond acceptor in Q69E Fe^{2+}SOD.

The 1.1 Å-resolution crystal structure also showed that H-bonds throughout the network involving Glu69 are shorter than those in WT FeSOD. Thus, Glu69's H-bond with coordinated solvent is not only reversed relative to the analogous WT FeSOD H-bond but also significantly stronger (2.8 Å in Q69E Fe^{2+}SOD vs 3.4 Å in WT Fe^{2+}SOD).[41] The strong redox tuning effect of residue 69's H-bond can therefore be understood in terms of its modifying the chemical nature of a first sphere ligand, from solvent with substantial imposed OH^- nature to solvent with strongly favored H_2O nature.

Thus, based on a variety of spectroscopic techniques, anion-binding and pH titrations, and the highest-resolution crystal structure to date of a FeSOD, we find that His69 does not impose H-bond donation on coordinated solvent and may even accept an H-bond in the reduced state, whereas Glu69 is likely neutral in the oxidized state, becoming anionic upon Fe reduction and thus (1) making a proton available for acquisition by coordinated solvent and (2) becoming a *strong obligate H-bond acceptor*. Based on literature p*K*'s and strengths of H-bonds, in conjunction with the measured E_m tuning loss observed in Q69H FeSOD, we were able to assess the competence of these factors to explain the very high E_m of Q69E FeSOD, obtaining an initial estimate that they could produce an approximately 700 mV increase in E_m.[41] Thus, although additional effects are not excluded, we find that strong stabilization of coordinated H_2O vs OH^- in addition to more favorable energetics of proton transfer to coordinated solvent are indeed capable of explaining the observed >660 mV increase in E_m for Q69E FeSOD.

Perspective

Labile protons are the liquid currency of proteins. Protonation changes the ligand natures of amino acids or coordinated solvent, thus providing proteins with a powerful means of modulating the reactivity of bound metal ions. Moreover the cost of doing so can be distributed among numerous residues and elements of the protein structure via H-bond networks. In addition, it is very common in biological chemistry for electron transfer to be coupled to proton transfer. For residues whose protonation state changes upon metal ion reduction, protein-mediated tuning of the p*K*'s modulates the E_m.

Water molecules provide special opportunities and are ideal molecular adaptors for coupling inorganic centers with biological macromolecules. H_2O is an inorganic molecule and can access the different properties of both the H_2O and the OH^- states under physiological conditions. Yet water is also the medium for which protein residues and structural elements have been selected by evolution. Bound H_2O and OH^-

favor different metal ions and different oxidation states, so proteins' ability to tune the p*K* of water molecules translates into ability to tune the E_m of the metal ion. Thus, coordinated solvent molecules should not automatically be dismissed simply as place-holders or labile coordination sites. While there are many sites in which they do appear spontaneously, we have presented compelling evidence that coordinated solvent can provide proteins with large leverage on the E_m and thus reactivity of bound metal ions.

We have produced variants of FeSOD with E_ms ranging over more than 900 mV, while preserving the structural integrity of the active site. This demonstrates the possibility of manipulating reactivity over a wide range and of generating sites with desired novel chemistry based on chemically rational design.

The work described herein was realized by numerous excellent students, postdoctoral fellows, and collaborators, whom I thank above all. I also acknowledge the excellent reviewers and competitors, who over the years have challenged me to refine my thinking and adhere to high standards.

BIOGRAPHICAL INFORMATION

A.-F. Miller obtained her Ph. D. in 1989 at Yale University and pursued postdoctoral work at MIT and at Brandeis University.

FOOTNOTES

* Tel: (859) 257-9349. Fax: (859) 323-1069. E-mail: afm@uky.edu. Current address: Francis Bitter Magnet Lab, Massachusetts Institute of Technology NW14, 150 Albany St., Cambridge MA 02139.

REFERENCES

1 Miller, A.-F.; Sorkin, D. L. Superoxide Dismutases: A Molecular Perspective. *Comments Mol. Cell. Biophys.* **1997**, *9*, 1–48.

2 Stallings, W. C.; Pattridge, K. A.; Strong, R. K.; Ludwig, M. L. Manganese and Iron Superoxide Dismutases are Structural Homologs. *J. Biol. Chem.* **1984**, *259*, 10695–10699.

3 Fink, R. C.; Scandalios, J. G. Molecular Evolution and Structure-Function Relationships of the Superoxide Dismutase Gene Families in Angiosperms and Their Relationship to Other Eukaryotic and Prokaryotic Superoxide Dismutases. *Arch. Biochem. Biophys.* **2002**, *399*, 19–36.

4 Pennington, C. D.; Gregory, E. M. Isolation and Reconstitution of Iron- and Manganese-Containing Superoxide Dismutase from *Bacteroides thetaiotaomicron*. *J. Bacteriol.* **1986**, *166*, 528–532.

5 Meier, B.; Barra, D.; Bossa, F.; Calabrese, L.; Rotilio, G. Synthesis of Either Fe- or Mn-Superoxide Dismutase with an Apparently Identical Protein Moiety by an Anaerobic Bacterium Dependent on the Metal Supplied. *J. Biol. Chem.* **1982**, *257*, 13977–13980.

6 Lah, M. S.; Dixon, M. M.; Pattridge, K. A.; Stallings, W. C.; Fee, J. A.; Ludwig, M. L. Structure-Function in *Escherichia coli* Iron Superoxide Dismutase: Comparisons with the Manganese Enzyme from *Thermus thermophilus*. *Biochemistry* **1995**, *34*, 1646–1660.

7 Bull, C.; Fee, J. A. Steady-State Kinetic Studies of Superoxide Dismutases: Properties of the Iron Containing Protein from *Escherichia coli*. *J. Am. Chem. Soc.* **1985**, *107*, 3295–3304.

8 Miller, A.-F.; Padmakumar, K.; Sorkin, D. L.; Karapetian, A.; Vance, C. K. Proton-Coupled Electron Transfer in Fe-Superoxide Dismutase and Mn-Superoxide Dismutase. *J. Inorg. Biochem.* **2003**, *93*, 71–83.

9 Stallings, W. C.; Metzger, A. L.; Pattridge, K. A.; Fee, J. A.; Ludwig, M. L. Structure-Function Relationships in Iron and Manganese Superoxide Dismutases. *Free Radical Res. Commun.* **1991**, *12* (13), 259–268.

10 Li, J.; Fisher, C. L.; Konecny, R.; Bashford, D.; Noodleman, L. Density Functional and Electrostatic Calculations of Manganese Superoxide Dismutase Active Site Complexes in Protein Environments. *Inorg. Chem.* **1999**, *38*, 929–939.

11 Edwards, R. A.; Baker, H. M.; Jameson, G. B.; Whittaker, M. M.; Whittaker, J. W.; Baker, E. N. Crystal Structure of *Escherichia coli* Manganese Superoxide Dismutase at 2.1-Å Resolution. *J. Biol. Inorg. Chem.* **1998**, *3*, 161–171.

12 Carlioz, A.; Ludwig, M. L.; Stallings, W. C.; Fee, J. A.; Steinman, H. M.; Touati, D. Iron Superoxide Dismutase. Nucleotide Sequence of the Gene from *Escherichia coli* K12 and Correlations with Crystal Structures. *J. Biol. Chem.* **1988**, *263*, 1555–1562.

13 Parker, M. W.; Blake, C. C. F. Iron- and Manganese-Containing Superoxide Dismutase can be Distinguished by Analysis of their Primary Structures. *FEBS Lett.* **1988**, *229*, 377–382.

14 Ose, D. E.; Fridovich, I. Reversible Removal of Manganese and its Substitution by Cobalt, Nickel or Zinc. *J. Biol. Chem.* **1976**, *251*, 1217–1218.

15 Ose, D. E.; Fridovich, I. Manganese-Containing Superoxide Dismutase from *Escherichia coli*: Reversible Resolution and Metal Replacements. *Arch. Biochem. Biophys.* **1979**, *194*, 360–364.

16 Brock, C. J.; Harris, J. I. Superoxide Dismutase from *Bacillus stearothermophilus*: Reversible Removal of Manganese and its Replacement by other Metals. *Biochem. Soc. Trans.* **1977**, *5*, 1537–1539.

17 Yamakura, F.; Suzuki, K. Cadmium, Chromium, and Manganese Replacement for Iron in Iron-Superoxide Dismutase from *Pseudomonas ovalis*. *J. Biochem. (Tokyo)* **1980**, *88*, 191–196.

18 Yang, M.; Cobine, P. A.; Molik, S.; Naranuntarat, A.; Lill, R.; Winge, D. R.; Culotta, V. C. The effects of mitochondrial iron homeostasison cofactor specificity of superoxide dismutase 2. *EMBO J.* **2006**, *25*, 1775–1783.

19 Vance, C. K.; Miller, A.-F. A simple proposal that can explain the inactivity of metal-substituted superoxide dismutases. *J. Am. Chem. Soc.* **1998**, *120*, 461–467.

20 Dean, J. A., Ed. *Lange's Handbook of Chemistry*,13 ed.; McGraw-Hill: New York, 1985.

21 Stein, J.; Fackler, J. P.; McClune, G. J.; Fee, J. A.; Chan, L. T. Superoxide and Manganese(II). Reactions of Mn-EDTA and Mn-CyDTA Complexes with $O_2^{\bullet-}$. X-ray structure of KMnEDTA · $2H_2O$. *Inorg. Chem.* **1979**, *18*, 3511–3519.

22 Gupta, R.; Borovik, A. S. Monomeric $Mn^{III/II}$ and $Fe^{III/II}$ complexes with Terminal Hydroxo and Oxo Ligands: Probing Reactivity via O-H Bond Dissociation Energies. *J. Am. Chem. Soc.* **2003**, *125*, 13234–13242.

23 Barrette, J.; W, C.; Sawyer, D. T.; Fee, J. A.; Asada, K. Potentiometric Titrations and Oxidation-Reduction Potentials of Several Iron Superoxide Dismutases. *Biochemistry* **1983**, *22*, 624–627.

24 Vance, C. K.; Miller, A.-F. Novel Insights into the Basis for *E. coli* SOD's Metal Ion Specificity, From Mn-Substituted Fe-SOD and Its Very High E_m. *Biochemistry* **2001**, *40*, 13079–13087.

25 Yikilmaz, E.; Rodgers, D. W.; Miller, A.-F. The crucial Importance of Chemistry in the Structure-Function Link: Manipulating Hydrogen Bonding in Iron-Containing Superoxide Dismutase. *Biochemistry* **2006**, *45*, 1151–1161.

26 Lévêque, V. J.-P.; Vance, C. K.; Nick, H. S.; Silverman, D. N. Redox Properties of Human Manganese Superoxide Dismutase and Active-Site Mutants. *Biochemistry* **2001**, *40*, 10586–10591.

27 Vance, C. K.; Miller, A.-F. Spectroscopic Comparisons of the pH dependencies of Fe-Substituted-(Mn) Superoxide Dismutase and Fe-Superoxide Dismutase. *Biochemistry* **1998**, *37*, 5518–5527.

28 Yamakura, F.; Matsumoto, T.; Kobayashi, K. In *Frontiers of Reactive Oxygen Species in Biology and Medicine*; Asada, K., Yoshikawa, T. Eds.; Elsevier science: Amsterdam, 1994; pp 115–118..

29 Whittaker, M. M.; Whittaker, J. W. Mutagenesis of a Proton Linkage Pathway in *Escherichia coli* Manganese Superoxide Dismutase. *Biochemistry* **1997**, *36*, 8923–8931.

30 Edwards, R. A.; Whittaker, M. M.; Whittaker, J. W.; Jameson, G. B.; Baker, E. N. Distinct Metal Environment in Fe-Substituted Manganese Superoxide Dismutase Provides a Structural Basis of Metal Specificity. *J. Am. Chem. Soc.* **1998**, *120*, 9684–9685.

31 Bertini, I.; Luchinat, C. *NMR of Paramagnetic Molecules in Biological Systems*; Benjamin/Cummings: New York, 1986.

32 LaMar, G. N.; Horrocks, W. D. Jr.; Holm, R. H. *NMR of Paramagnetic molecules.*; Academic Press; New York. 1973.

33 (a) Grove, L. E.; Xie, J.; Yikilmaz, E.; Miller, A.-F.; Brunold, T. C. Spectroscopic and Computational Investigation of Second-Sphere Contributions to Redox Tuning in *Eschericia coli* Iron Superoxide Dismutase. *Inorg. Chem.* **2008**, in press. (b) Grove, L. E.; Xie, J.; Yikilmaz, E.; Karapetyan, A.; Miller, A.-F.; Brunold, T. C. Spectroscopic

and Computational Insights into Second-Sphere Amino-Acid Tuning of Substrate Analogue/Active-Site Interactions in Iron(III) Superoxide Dismutase. *Inorg. Chem.* **2008**, in press.

34 Tabares, L. C.; Cortez, N.; Hiraoka, B. Y.; Yamakura, F.; Un, S. Effects of Substrate Analogues and pH on Manganese Superoxide Dismutases. *Biochemistry* **2006**, *45*, 1919–1929.

35 Maliekal, J.; Karapetian, A.; Vance, C.; Yikilmaz, E.; Wu, Q.; Jackson, T.; Brunold, T. C.; Spiro, T. G.; Miller, A.-F. Comparison and Contrasts between the Active Site pKs of Mn-Superoxide Dismutase and Those of Fe-Superoxide Dismutase. *J. Am. Chem. Soc.* **2002**, *124*, 15064–15075.

36 Baldwin, M. J.; Pecoraro, V. L. Energies of Proton-Coupled Electron Transfer in High-Valent $Mn_2(\mu\text{-}O)_2$ Systems: Models for Water Oxidation by the Oxygen-Evolving Complex of Photosystem II. *J. Am. Chem. Soc.* **1996**, *118*, 11325–11326.

37 Fisher, C. L.; Chen, J.-L.; Li, J.; Bashford, D.; Noodleman, L. Density Functional and Electrostatic Calculations for a Model of a Manganese Superoxide Dismutase Active Site in Aqueous Solution. *J. Phys. Chem.* **1996**, *100*, 13498–13505.

38 Wintjens, R.; Gilis, D.; Rooman, M. Mn/Fe Superoxide Dismutase Interaction Fingerprints and Prediction of Oligomerization and Metal Cofactor from Sequence. *Proteins: Struct., Funct., Bioinf.* **2008**, *70*, 1564–1577.

39 Vance, C. K.; Kang, Y. M.; Miller, A.-F. Selective ^{15}N Labeling and Direct Observation by NMR of the Active Site Glutamine of Fe-Containing Superoxide Dismutase. *J. Biomol. NMR* **1997**, *9*, 201–206.

40 Schwartz, A. L.; Yikilmaz, E.; Vance, C. K.; Vathyam, S.; Koder, R. L., Jr.; Miller, A.-F. Mutational and Spectroscopic Studies of the Significance of the Active Site Gln to Metal Ion Specificity in Superoxide Dismutase. *J. Inorg. Biochem.* **2000**, *80*, 247–256.

41 Yikilmaz, E.; Porta, J.; Grove, L. E.; Vahedi-Faridi, A.; Bronshteyn, Y.; Brunold, T. C.; Borgstahl, G. E. O.; Miller, A.-F. How Can a Single Second Sphere Amino Acid Substitution Cause Reduction Midpoint Potential Changes of Hundreds of Millivolts. *J. Am. Chem. Soc.* **2007**, *129*, 9927–9940.

42 Fee, J. A.; McClune, G. J.; Lees, A. C.; Zidovetzki, R.; Pecht, I. The pH Dependence of the Spectral and Anion Binding Properties of Iron Containing Superoxide Dismutase from *E. coli* B: An Explanation for the Azide Inhibition of Dismutase Activity. *Isr. J. Chem.* **1981**, *21*, 54–58.

43 Yikilmaz, E.; Xie, J.; Miller, A.-F.; Brunold, T. C. Hydrogen-Bond-Mediated Tuning of the Redox Potential of the Non-Heme Fe Site of Superoxide Dismutase. *J. Am. Chem. Soc.* **2002**, *124*, 3482–3483.

44 Baes, C. F., Jr.; Mesmer, R. E. *The Hydrolysis of Cations*; John Wiley & Sons: New York, 1976.

45 Sawyer, D. T.; Valentine, J. S. How Super Is Superoxide. *Acc. Chem. Res.* **1981**, *14*, 393–400.

46 Yamakura, F.; Kobayashi, K.; Ue, H.; Konno, M. The pH-Dependent Changes of the Enzymic Activity and Spectroscopic Properties of Iron-Substituted Manganese Superoxide Dismutase. *Eur. J. Biochem.* **1995**, *227*, 700–706.

47 DeLano, W. L. The PyMOL Molecular Graphics System http://www.pymol.org, 2002, DeLano Scientific.